

# TWO TYPES OF C(A)SH IN THE HARDENED CEMENT PASTES USING LOW HEAT / ORDINARY PORTLAND CEMENT EVALUATED BY NITROGEN SORPTION

Ryo Kurihara\*<sup>1</sup>, Hiroki Sugimoto\*<sup>1</sup>, Ippei Maruyama\*<sup>2</sup>

## ABSTRACT

In this study, we reevaluated the Tennis and Jennings' model of two types of calcium silicate hydrates in Portland cement based on nitrogen sorption measurement on low heat / ordinary Portland cement with W/C ratio = 0.55. Optimized results indicate that the ratio of low-density C(A)SH to total amount of C(A)SH increases with progression of the hydration in the case of ordinary Portland cement. Whereas this ratio for low heat Portland cement paste increases until degree of hydration of cement gets around 0.6~0.7, then decreases at higher degree of hydration.

**Keywords:** calcium (alumino) silicate hydrate (C(A)SH), nitrogen sorption, BET surface area, XRD, Rietveld analysis

## 1. INTRODUCTION

Shrinkage of hardened cement paste (hcp) in concrete causes alteration of properties of concrete through micro-cracking around aggregate [1], also causes large drying shrinkage of concrete. When such shrinkage is restrained, cracking occurs. This cracking has large influence on the stiffness of structural response against earthquake [2].

It has been reported that calcium (alumino) silicate hydrate (C(A)SH) is the major hydration product of the cement paste, and the alteration of C(A)SH under drying greatly affects the property change of the cement paste [3]. In previous studies, from the observation by scanning electron microscope, two different morphologies of C(A)SH has been confirmed [4], and C(A)SH is divided into inner- and outer-product. Fonseca and Jennings observed that the morphology of outer-product changed significantly during drying [5]. Based on these observations, it is thought that this large morphology change of outer-product affects the irreversible change of the cement paste during first drying. On the other study, Tennis and Jennings proposed model of two types of C(A)SH defined by nitrogen sorption measurements (T-J model) [6,7]. This model is dividing C(A)SH forming in the cement paste with two different densities (i.e. different porosity), a high-density (HD) C(A)SH and a low-density (LD) C(A)SH, and both amounts can be quantified. The definitions of outer-product and LD C(A)SH are not exactly same, but they refer similar region of the C(A)SH in the paste.

Therefore, Quantifying the amount of LD C(A)SH of the paste is beneficial for understanding microstructure of hcp, and has a potential to improve the way predicting drying shrinkage or other physical

properties of hcp.

On the contrary, the previous research has reported that the drying shrinkage of cement paste differs by the mineral compositions of cement [8-10]. And these mechanisms are not clarified. Based on T-J model, understanding how much LD C(A)SH precipitates in the case of each type of cement is meaningful.

The aim of this paper is to clarify the evolution of amounts of two types of C(A)SH in the cement paste using different types of cement with time. Ordinary Portland cement and low heat Portland cement were used for the cement pastes, nitrogen sorption measurements and powder X-ray diffraction (XRD) measurements were conducted at certain age of the samples up to 1 year. The evolution of each type of C(A)SH was evaluated following T-J model.

## 2. T-J MODEL

In this model [6], the distribution of C(A)SH into two types is determined by assuming the LD C(A)SH is the only component of the microstructure measured by nitrogen. Both types of C(A)SH contain gel pores, HD C(A)SH has no porosity accessible to nitrogen, while only some part of pores in LD C(A)SH are accessible to nitrogen. Based on these assumptions, the ratio of the mass of LD C(A)SH to total mass of C(A)SH,  $M_r$  is calculated by Eq. 1:

$$M_r = (S_{N2}M_D)/(S_{LD}M_t) \quad (1)$$

where  $S_{N2}$  ( $m^2/g$ ) is the specific surface area of the dried cement paste determined from nitrogen sorption measurements,  $M_D$  (g) is the mass of dried cement paste,  $S_{LD}$  is the specific surface area of LD C(A)SH

\*1 Graduate student, Dept. of Environmental Engineering and Architecture, Nagoya Univ., JCI Student Member

\*2 Professor, Graduate School of Environmental Engineering and Architecture, Nagoya Univ., Dr.Eng., JCI Member

(m<sup>2</sup>/g-dried LD C(A)SH, it is not directly measurable), and  $M_t$  (g) is the total mass of C(A)SH which can be quantified by XRD and Rietveld analysis.

The volume of HD C(A)SH and LD C(A)SH is given by Eq. 2, Eq. 3:

$$V_{HD} = M_t - (M_r M_t) / \rho_{HD} \quad (2)$$

$$V_{LD} = M_r M_t / \rho_{LD} \quad (3)$$

where  $V_X$  (cm<sup>3</sup>) is the volume of HD / LD C(A)SH,  $\rho_{HD}$  and  $\rho_{LD}$  (g/cm<sup>3</sup>) are the density of HD / LD C(A)SH. Note that in this condition, C(A)SH is dried and assumed to have no water in its pores, but  $V_{HD}$  and  $V_{LD}$  include the empty pores existed in each C(A)SH.

The additional volume of pores in LD C(A)SH measurable by nitrogen sorption is given by Eq. 4:

$$V_p = V_{LD} - M_r M_t / \rho_{HD} \quad (4)$$

where  $V_p$  (cm<sup>3</sup>) is the volume of porosity of LD C(A)SH, this is the volume of porosity in the C(A)SH that is accessible to nitrogen molecules.

Thus, except for the values of  $S_{LD}$ ,  $\rho_{HD}$ , and  $\rho_{LD}$ , all the parameters can be obtained from experiments. The values remaining to be determined are the fitting parameters for this model.

### 3. EXPERIMENTAL PROCEDURE

#### 3.1 Materials and sample preparation

Low heat Portland cement (notation: L) and ordinary Portland cement (notation: N) were used for the cement paste specimens. The chemical compositions and the mineral compositions of both Portland cement are listed in Table 1 and Table 2. The mineral composition was determined by XRD measurements and Rietveld analysis.

The cement pastes using low heat / ordinary Portland cement were set the water to cement ratio as 0.55, named L55 and N55, respectively. All the materials were stored in a thermostatic chamber at  $20 \pm 1$  °C for 1 day prior to mixing. The paste was mixed in a planetary centrifugal mixer (the rotation / revolution speed is 980, 1000 rpm, respectively.) for 1.5 min after the water was added to achieve W/C = 0.40. After first mixing, the remaining water was added to get W/C =

0.55, and further mixing was conducted for 1.5 min. Whole mixing was performed at room temperature, after mixing, fresh paste was immediately moved to a temperature control room. In order to minimize segregation, the paste was remixed every 30 min until almost no bleeding was observed (approximately 6 ~ 10 hours after mixing). After remixing, the specimens were casted into molds with tightly sealed condition at  $20 \pm 1$  °C. They were cured until the ages of each measurement. For L55, the ages of measurements are 3, 7, 14, 28, 56, 91, 182 and 364 days, in the case of N55, these are 3, 7, 28, 91, 182, 364 days. At each curing period, the nitrogen sorption measurements and stopping hydration processes for XRD measurements were conducted.

#### 3.2 Experimental selection

##### (1) XRD / Rietveld analysis

The specimens were analyzed by powder X-ray diffractometer (D8 advance, Bruker AXS) after each curing periods. All the specimens were crushed into 2 mm pieces or smaller with a hammer and immersed in isopropanol for 30 min, then the sample and isopropanol were separated by suction filtration. After that, the immersion in isopropanol for further 6 hours and the filtration were conducted again. After the hydration stoppage by isopropanol, the samples were conditioned for 2 weeks at a constant temperature of  $20 \pm 1$  °C in a desiccator using circulated air scrubbed with a CO<sub>2</sub> absorbent and a saturated LiCl aqueous solution (11% RH). After conditioning, the samples were ground in a ball mill and graded with a 90 μm sieve, and only the powder that passed through the sieve was used for the various measurements. XRD measurements were conducted under the following instrument conditions: Cu-Kα X-ray source, 40 kV tube voltage, 40 mA tube current,  $2\theta = 2\sim 65^\circ$  scanning range, 0.02° step width, and 0.5°/min scanning speed. The samples whose hydration was stopped and then underwent humidity conditioning were admixed with 10 wt% corundum (α-Al<sub>2</sub>O<sub>3</sub>) as an internal standard. Rietveld analysis was done for the entire measured spectrum using the TOPAS ver. 4.2 software (Bruker AXS). Alite (C<sub>3</sub>S), belite (C<sub>2</sub>S), aluminat phase (C<sub>3</sub>A), ferrite phase (C<sub>4</sub>AF), periclase (MgO), gypsum (CaSO<sub>4</sub>·2H<sub>2</sub>O), bassanite (CaSO<sub>4</sub>·0.5H<sub>2</sub>O), anhydrite (CaSO<sub>4</sub>), portlandite (Ca(OH)<sub>2</sub> (CH)), ettringite (C<sub>3</sub>A·3CaSO<sub>4</sub>·32H<sub>2</sub>O), monosulfate

Table 1 Chemical composition of low heat / ordinary Portland cement

	Ig.loss	SiO <sub>2</sub>	Al <sub>2</sub> O <sub>3</sub>	Fe <sub>2</sub> O <sub>3</sub>	CaO	MgO	SO <sub>3</sub>	Na <sub>2</sub> O	Na <sub>2</sub> Oeq	K <sub>2</sub> O
	(%)	(%)	(%)	(%)	(%)	(%)	(%)	(%)	(%)	(%)
L	0.73	25.85	3.32	3.08	62.28	0.76	2.84	0.19	0.35	0.25
N	0.37	21.02	5.67	3.46	64.67	1.26	2.32	0.28	0.50	0.34

Table 2 Mineral composition of white cement determined by XRD and Rietveld analysis

	C <sub>3</sub> S	C <sub>2</sub> S	C <sub>3</sub> A	C <sub>4</sub> AF	Periclase	Bassanite	Gypsum	Anhydrite
	(%)	(%)	(%)	(%)	(%)	(%)	(%)	(%)
L	20.58±1.56	62.17±3.18	2.13±0.22	10.7±0.58	0.491±0.17	2.45±0.61	1.47±0.18	-
N	49.20±0.62	30.01±1.86	5.50±0.21	11.52±0.14	1.65±0.51	-	1.08±0.08	1.04±0.15

( $C_3A \cdot CaSO_4 \cdot 12H_2O$ ), hydrogarnet ( $C_3AH_6$ ), hemicarboaluminate ( $C_4A \cdot 0.5CO_2 \cdot 12.5H_2O$ ), and monocarbonate ( $C_4A \cdot CO_2 \cdot 12H_2O$ ), as clinker minerals and cement hydration products, were chosen to be quantified. The details of the XRD/Rietveld analysis are described in our previous paper [11,12]. Three samples were measured at each condition. In the phase calculation process, all Fe atoms in the amorphous phases were considered to belong to  $C_4FH_{13}$  at 11% RH, and all Al and Si atoms in amorphous phases were considered to be in C(A)SH.

## (2) Nitrogen sorption test

Nitrogen sorption measurements were performed by the volumetric method using a nitrogen sorption analyzer (BELSORP-mini II, MicrotracBEL Corp.). A sample (~ 100 mg) was used for each measurement at  $-196^\circ C$ , with a sorption tolerance of  $5.0 \text{ cm}^3/\text{g}$  and a time tolerance of 180 sec. The measurement points on the adsorption and desorption branches were ended at  $p/p_0 = 0.99$ . The specific surface area ( $S_{N_2}$ ) of adsorption branch was calculated using the BET theory [13] with a nitrogen molecule section value of  $0.162 \text{ nm}^2$  [14].

The samples were crushed, and powder with a particle size of 25 to  $75 \mu\text{m}$  was used for this analysis. For pre-treatment, the samples were dried using a vacuum pump (theoretical minimum pressure of  $6.7 \times 10^{-2} \text{ Pa}$ ) at room temperature for 3 hours; this led to the very dry initial state. After completed measurements, the samples were dried using same vacuum pump at  $105^\circ C$  with a heating mantle for 30 min in order to get the mass of dried cement paste (i.e. no evaporable water was included). All the sorption isotherms were normalized by the mass of the samples dried at  $105^\circ C$  mentioned above.

## 4. RESULTS AND DISCUSSIONS

### (1) Degree of hydration

Figure. 1 and Fig. 2 show degrees of hydration for L55 and N55. In the figure, the led filled triangle legend refers the total hydration degree for all mineral components. For both cases, alite and aluminate phase are almost fully hydrated until 28 days.

### (2) Nitrogen surface area

Figure. 3 shows calculated surface area ( $S_{N_2}$ ) from nitrogen sorption with respect to curing periods. In the case of N55, the value of  $S_{N_2}$  increases with age. On the other hand, the  $S_{N_2}$  of L55 increases until 28 days, and gets almost constant after 28 days or more. The hydration of alite is almost completed in both cases at aged 28 days, so the additional precipitation of C(A)SH is thought to be derived from reaction of belite after 28 days of age. Therefore, in the case of low heat Portland cement, it is revealed that the nitrogen surface area is not increased by the reaction of belite which progresses after almost finished the reaction of alite.

### (3) Optimization

For the nitrogen sorption measurement, pre-treatment of a specimen prior to measurement is necessary and this drying always accompanies the microstructural change of the hardened cement paste. We already reported the duration or temperature of

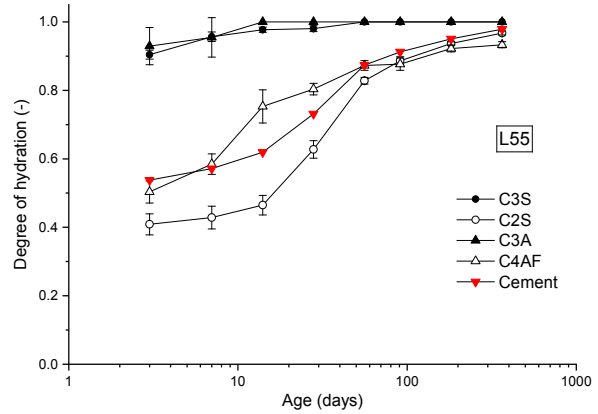


Fig. 1 Degrees of hydration of each cement minerals against material age (L55)

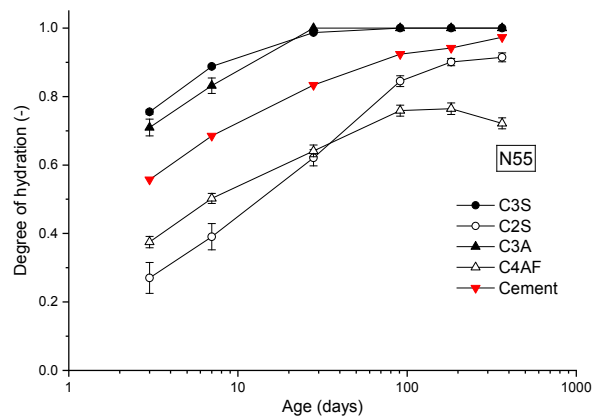


Fig. 2 Degrees of hydration of each cement minerals against material age (N55)

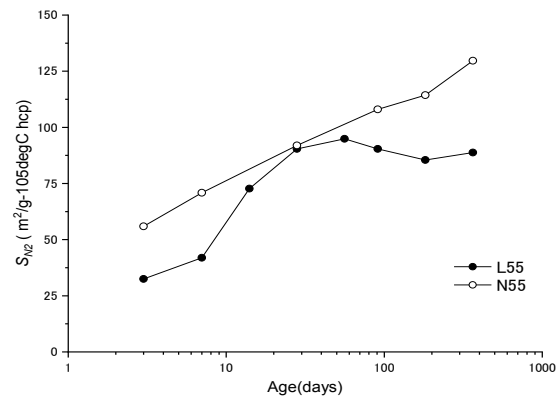


Fig. 3 The result of measured  $S_{N_2}$ , nitrogen surface area against material age.

pre-treatment significantly affects the measured sorption isotherm and surface area [15, 16]. In this study, we applied a vacuum drying at room temperature as pre-treatment for sorption measurement, and it is a different protocol as applied in the T-J model (i.e. D-drying). For N55 at the age of 6 months, we obtained  $114 \text{ m}^2/\text{g}$ -dried paste. This value is different from  $68.5$  and  $70.9 \text{ m}^2/\text{g}$ -D-dried paste of the cement paste which W/C ratio is  $0.501$  [18]. There is a significant difference between these obtained results, so we considered our applied protocol described above can preserve the original microstructure before

pre-treatment. Based on obtained results, reevaluation of T-J model was conducted for the case of two different Portland cement. Regarding Eq. 1 – 4, the fitting parameters are  $S_{LD}$ ,  $\rho_{HD}$ ,  $\rho_{LD}$ . An iterative process has been used to optimize the values of  $S_{LD}$ ,  $\rho_{HD}$ , and  $\rho_{LD}$  based on the fit between measured values for surface area ( $S_{N2}$ ) and porosity ( $V_p$ , shown in Eq. 4), both measured by nitrogen sorption, and the values calculated by T-J model. The criterion for determining fitting is the P-value in the statistics. When the measured  $V_p$  and the calculated  $V_p$  are linearly approximated by  $y = ax$ , this P-value is the significance probability for the null hypothesis that  $a = 1$ . This P-value is ranging between 0 and 1. The higher P-value close to 1 indicates better fit between experimental values and calculated values. For the experimental values for porosity accessible to nitrogen ( $V_p$ ), the adsorption amounts at  $p/p_0 = 0.90$  in adsorption branches are used. At this  $p/p_0$ , pores up to about 20 nm in diameter (assuming a cylindrical shape) are filled, and we assumed that all pores in LD C(A)SH accessible to nitrogen are filled in this point.

Figures. 4 - 6 show the P-value with respect to each fitting parameter (i.e.  $S_{LD}$ ,  $\rho_{HD}$ , and  $\rho_{LD}$ , respectively), the plots of calculated and measured values for  $V_p$  in both cases of L55 and N55 are shown in Fig. 7 and Fig. 8. The optimized values for each parameter are listed in Table 3. Comparing our values and literature values reported by Tennis and Jennings, the  $S_{LD}$  of our results are higher than reported value in both cases of L55, N55. In addition, the  $\rho_{LD}$  of our results are smaller than literature value. The values of  $\rho_{LD}$  and  $\rho_{HD}$  include empty pores, and for instance, the value of 2.5 g/cm<sup>3</sup> is used for the density of C-S-H exclusive of pores [18], LD C(A)SH contains 54% porosity (L55), 51% (N55), and 42% (TJ model). On the other hands, each porosity of HD C(A)SH of L55 and N55 is smaller than T-J model. When these porosities are filled with water, the saturated density of C(A)SH can be calculated. Average value of the saturated density for L55 is 1.88 g/cm<sup>3</sup>, and that for N55 is 1.85 g/cm<sup>3</sup>.

From the above, the ratios of the mass of LD C(A)SH to the total mass of C(A)SH ( $M_r$ ) with respect to the degree of hydration of cement is plotted in Fig. 9. In the case of N55, the value of  $M_r$  increases with progression of hydration. This trend is similar as reported results of the cement paste with W/C = 0.50 [6]. But in the case of L55, it clearly shows a different trend; 1) the value of  $M_r$  increases until degree of hydration gets 0.6 (aged 14 days), 2)  $M_r$  gets almost constant until degree of hydration is 0.73 (28 days), 3)  $M_r$  decreases in the further hydration process.

Combining the results of  $M_r$  and the phase compositions calculated from Rietveld analysis, the relative volume compositions of each phases at conditioned at 105 °C with respect to hydration degree are shown in Fig. 10 and Fig. 11.

It is clarified that based on T-J model, which dividing of C(A)SH into LD and HD regions defined by nitrogen sorption measurements, the evolutions of the ratio of low-density region of C(A)SH to whole

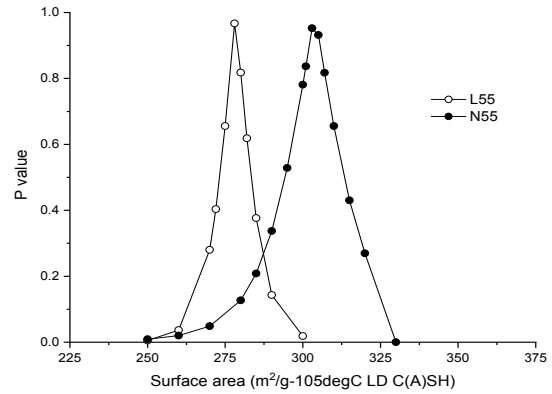


Fig. 4 The results of P-values for different  $S_{LD}$

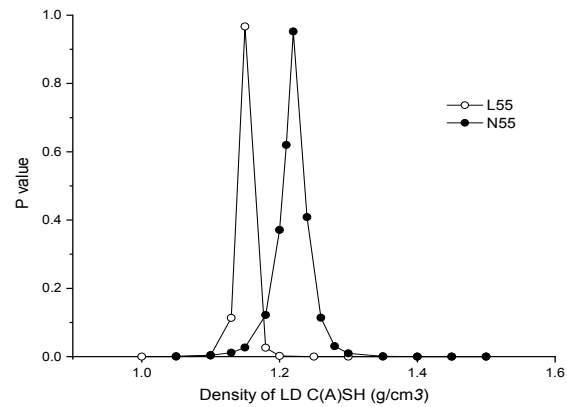


Fig. 5 The results of P-values for different  $\rho_{LD}$

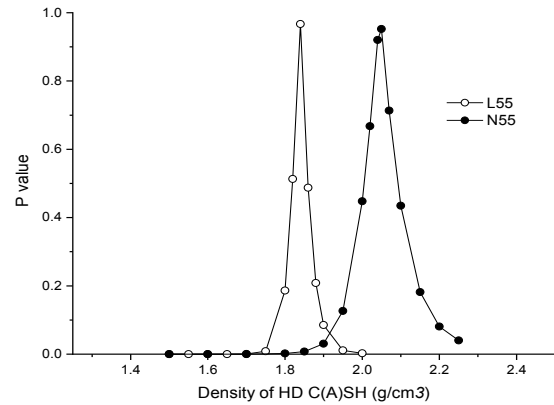


Fig. 6 The results of P-values for different  $\rho_{HD}$

C(A)SH with material ages or degree of hydration are different between low heat / ordinary Portland cement. If evaluating shrinkage behavior or other mechanical properties of different types of cement through this T-J model, it is necessary for making it clear how the ratio of low-density C(A)SH changes.

## 5. CONCLUSIONS

The model for two types of C(A)SH in the microstructure of hardened cement pastes is reevaluated in the case of ordinary Portland cement and low heat Portland cement. Nitrogen sorption measurements and XRD / Rietveld analysis were performed with hardened

cement pastes (W/C = 0.55) at specific age from 3 to 364 days. The followings were newly obtained by the experiment:

- (1) The surface area measured by nitrogen sorption increases with the progression of hydration in the case ordinary Portland cement, while for low heat Portland cement, this surface area increases until 28 days and gets almost constant after 28 days of age. This tendency is linked to the reactions of alite and belite, the hydration of belite which progresses after almost fully hydration of alite does not increase nitrogen surface area in the case low heat Portland cement.
- (2) Based on the calculated results, the ratios of the mass of LD C(A)SH to the total mass of C(A)SH show different trend between low heat / ordinary Portland cement. In the case of ordinary Portland cement, this ratio increases with degree of hydration. As for low heat Portland cement paste, this ratio increases until around degree of hydration achieves 0.6 ~ 0.7, then decreases with further progression of hydration.

#### ACKNOWLEDGEMENT

This research is supported by Chubu Electric Power Co. Inc., and JSPS KAKENHI 18H03804, Grant-in-Aid for JSPS Research Fellow 17J11519. Authors express their acknowledgements.

#### REFERENCES

- [1] I. Maruyama et al., "Strength and Young's modulus change in concrete due to long-term drying and heating up to 90 °C," *Cement and Concrete Research*, Vol. 66, 2014, pp. 48-63.
- [2] I. Maruyama, "Multi-scale Review for Possible Mechanisms of Natural Frequency Change of Reinforced Concrete Structures under an Ordinary Drying Condition," *Journal of Advanced Concrete Technology*, Vol. 14, 2016, pp. 691-705.
- [3] I. Maruyama et al., "Microstructural and bulk property changes in hardened cement paste during the first drying process," *Cement and Concrete Research*, Vol. 58, 2014, pp. 20-34.
- [4] S. Goto et al., "Composition and Morphology of Hydrated Tricalcium Silicate," *Journal of the American Ceramic Society*, Vol. 59, No. 7-8, 1976, pp. 281-284.
- [5] P. C. Fonseca, H. M. Jennings, "The effect of drying on early-age morphology of C-S-H as observed in environmental SEM," *Cement and Concrete Research*, Vol. 40, 2010, pp. 1673-1680.
- [6] P. D. Tennis, H. M. Jennings, "A model for two types of calcium silicate hydrate in the microstructure of Portland cement pastes," *Cement and Concrete Research*, Vol. 30, 2000, pp. 855-863.
- [7] H. M. Jennings, P. D. Tennis, "Model for the developing microstructure in Portland cement pastes," *Journal of the American Ceramic Society*, Vol. 77, No. 12, 1994, pp. 3161-3172.

Table 3 The determined values of  $S_{LD}$ ,  $\rho_{LD}$ ,  $\rho_{HD}$

	$S_{LD}$ ( $m^2/g$ )	$\rho_{LD}$ ( $g/cm^3$ )	$\rho_{HD}$ ( $g/cm^3$ )
L55	278	1.15	1.84
N55	303	1.22	2.05
T-J model [6]	247	1.44	1.75

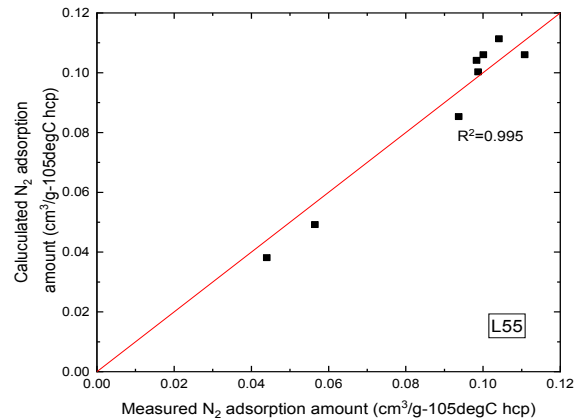


Fig. 7 The calculated and measured values of volume of porosity measured by nitrogen sorption (L55). The red line represents  $y = x$ .

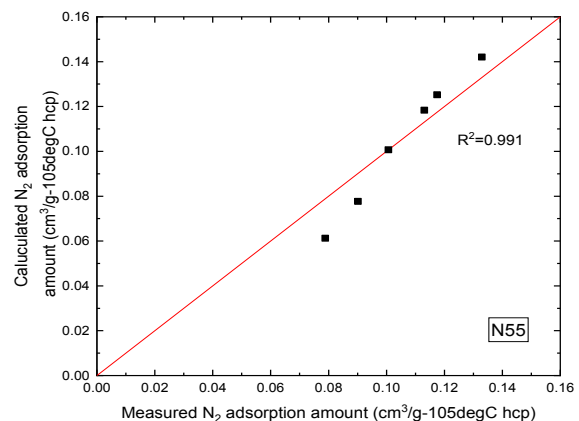


Fig. 8 The calculated and measured values of volume of porosity measured by nitrogen sorption (N55). The red line represents  $y = x$ .

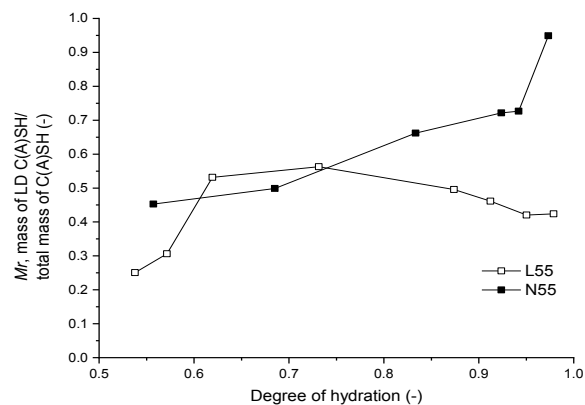


Fig. 9 The ratio of the mass of LD C(A)SH to the total mass of C(A)SH with the degree of hydration of cement

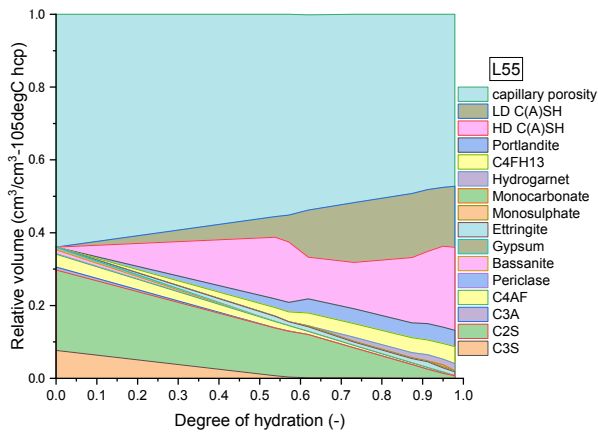


Fig. 11 Relative volume compositions of 105 °C cement paste (L55)

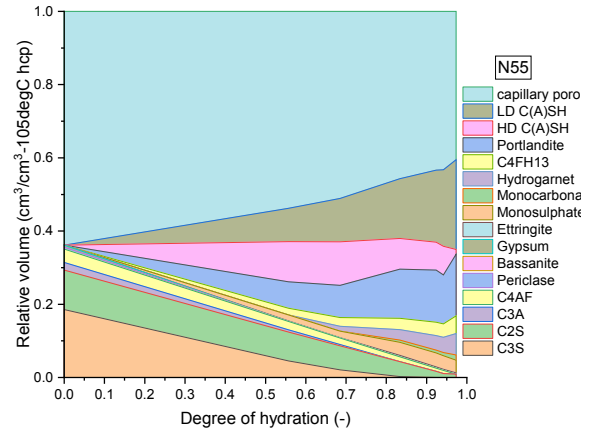


Fig. 10 Relative volume compositions of 105 °C cement paste (N55)

- [8] I. Maruyama, "Origin of drying shrinkage of hardened cement paste: Hydration pressure," *Journal of Advanced Concrete Technology*, Vol. 8, 2010, pp. 187-200.
- [9] T. Haji et al., "Impact of demolding age and mineral composition of cement on drying shrinkage of cement paste," *Proceedings of Japan Concrete Institute*, Vol. 38, 2016, pp. 45-50.
- [10] H. Nakayama et al., "Study of shrinkage strain of hardened cement using different Portland cements," *Cement Science and Concrete Technology*, Vol. 70, 2016, pp. 252-259.
- [11] I. Maruyama, G. Igarashi, "Cement reaction and resultant physical properties of cement paste," *Journal of Advanced Concrete Technology*, Vol. 12, 2014, pp. 200-213.
- [12] I. Maruyama, G. Igarashi, "Numerical Approach towards Aging Management of Concrete Structures: Material Strength Evaluation in a Massive Concrete Structure under One-Sided Heating," *Journal of Advanced Concrete Technology*, Vol. 13, 2015, pp. 500-527.
- [13] S. Brunauer, P. H. Emmett and E. Teller, "Adsorption of Gases in Multimolecular Layers," *Journal of the American Chemical Society*, Vol. 60, 1938, pp. 309-319.
- [14] A. L. McClellan, H. F. Harnsberger, "Cross-sectional of molecules adsorbed on solid surface," *Journal of Colloid interface Science*, Vol. 23, 1967, pp. 577-599.
- [15] H. Sugimoto et al., "Fundamental study for the impact of the methods of hydration stoppage and pre-treatment on sorption measurement," *Proceedings of Japan Concrete Institute*, Vol. 39, 2017, pp. 427-432. (in Japanese)
- [16] I. Maruyama et al., "Alteration of Sorption Properties of Hardened Cement Paste under Drying Process," *Journal of the Society of Material Science*, Vol. 62, No. 3, 2013, pp. 219-223
- [17] C.M. Hunt, "Nitrogen sorption measurements and surface areas of hardened cement pastes, Proc of a Symp on the Structure of Portland Cement Paste and Concrete," *Highway Res. Board Sp. Rep. 90*, National Academy of Engineering, Washington, DC, 1966, pp. 112-122.
- [18] H.F.W. Taylor, "Cement Chemistry 2nd edition," Thomas Telford, London, 1997.